Electronic Supplementary Information (ESI): Role of disorder in limiting the true multi-electron redox in ε-$LiVOPO_4$

Jatinkumar Rana,[a] Yong Shi,[a], Mateusz J. Zuba,[a] Kamila M. Wiaderek,[b] Jun Feng,[a] Hui Zhou,[a] Jia Ding,[a] Tianpin Wu,[b] Giannantonio Cibin,[c] Mahalingam Balasubramanian,[b] Fredrick Omenya,[a] Natasha Chernova,[a] Karena W. Chapman,[d] M. Stanley Whittingham[a] and Louis F. J. Piper*[a]

Beamline-specific details

Higher harmonics were suppressed by using the harmonic rejection mirrors at all beamlines, except at 5BM of APS where it was done by detunning the beam intensity to 60 % of the maximum intensity. An unfocussed beam of size ~1 mm × 1 mm at 18BM of DLS, ~3 mm × 1 mm at 5BM of APS, ~3 mm × 3 mm at 9BM of APS and ~5 mm × 1 mm at 20BM of APS was used. The size of the incident beam at each beamline was chosen so as to have the best possible energy resolution without sacrificing much of the beam intensity. The pre-edge region of the pristine ε-$LiVOPO_4$ measured at different beamlines (Figure S1) shows comparable energy resolution of these beamlines.

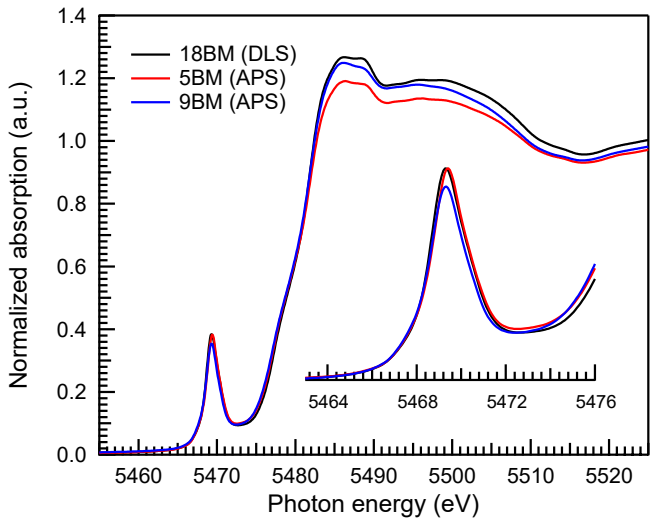

Fig. S1 Normalized V K-edge absorption spectra of the pristine ε-$LiVOPO_4$ sample measured at different beamlines. The pre-edge region in the inset shows comparable energy resolution of different beamlines used in this study.

[a] *NorthEast Center for Chemical Energy Storage (NECCES) at Binghamton University in Binghamton, NY, 13902, United States. E-mail: lpiper@binghamton.edu*
[b] *X-ray Science Division, Advanced Photon Source, Argonne National Laboratory, Argonne, Illinois 60439, United States.*
[c] *Diamond Light Source Ltd., Diamond House, Harwell Science and Innovation Campus, Didcot, Oxfordshire OX11 0DE, United Kingdom.*
[d] *Department of Chemistry, Stony Brook University, Stony Brook, New York 11974, United States.*

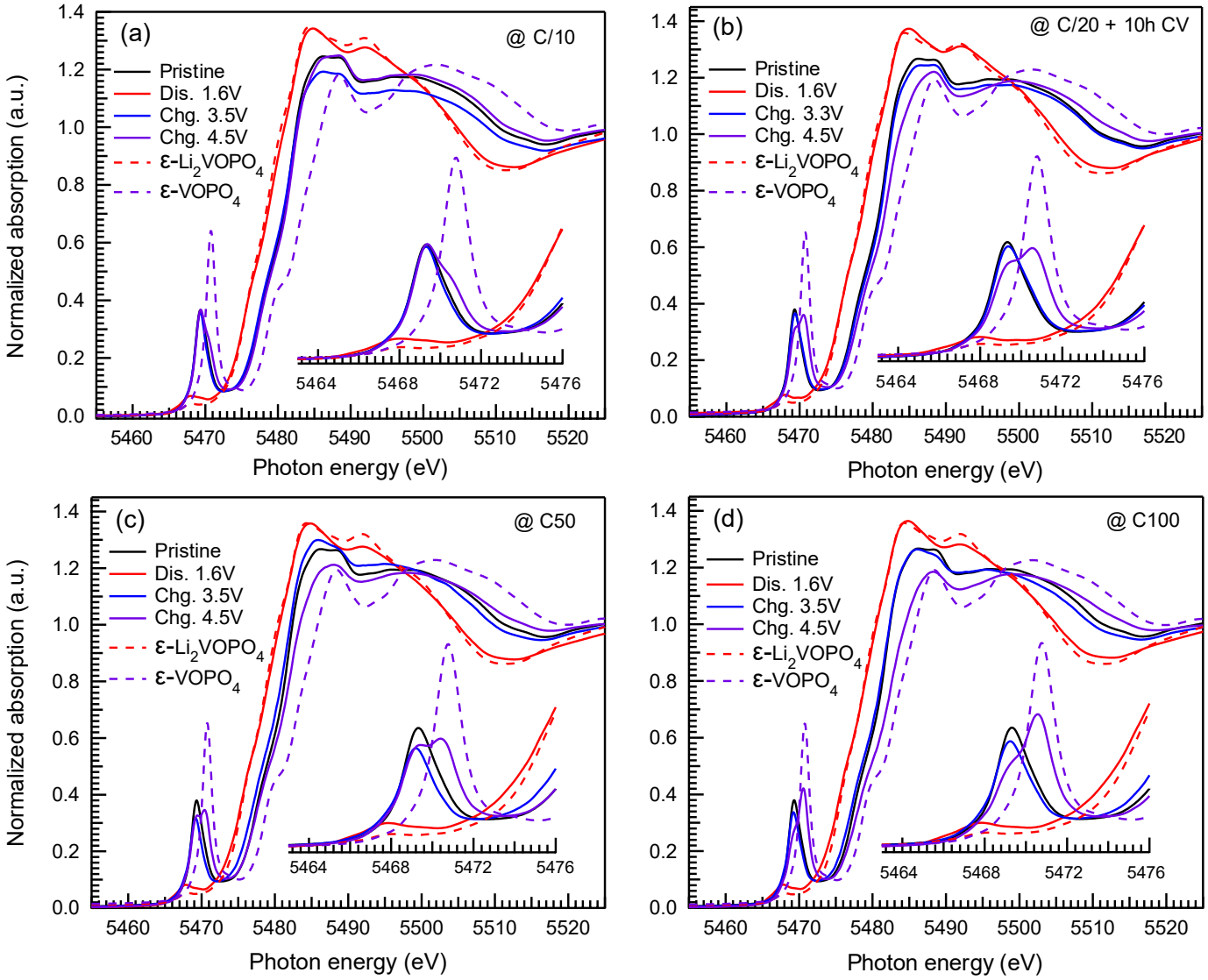

Fig. S2 Normalized V K-edge absorption spectra of ex-situ ε-$LiVOPO_4$ samples discharged/charged using different rates.

EXAFS analysis

Figure S3a shows EXAFS data of vanadyl phosphate reference compounds with the first prominent peak, representing the V-O coordination. ε-$LiVOPO_4$ has a triclinic structure (space group: $P\bar{1}$)[1], where V atoms are distributed over two octahedral sites. As a result, a theoretical model explaining EXAFS data of ε-$LiVOPO_4$ involved the sum of two FEFF calculations, averaging local environments around these two V sites as shown in Tables S1 and S2. Typical fitting parameters involved a single amplitude reduction factor (S_0^2)[2–4] and an overall energy parameter (ΔE_0)[4] for each dataset. In addition, a fractional change in the bond length (α) and a mean-squared relative displacement parameter (σ^2) were refined for each coordination shell depending on the type of backscattering atoms. Parameters for multiple-scattering paths were constrained in terms of those of the corresponding single-scattering paths as described elsewhere[5]. The reduced crystal symmetry of triclinic ε-$LiVOPO_4$ gives rise to local environments, where none of the bond lengths are degenerate (see Tables S1 and S2). The first coordination shell has six V-O bonds with short (1.626 Å to 1.627 Å), medium (1.945 Å to 2.099 Å) and long (2.240 Å) bond lengths. Best-fit to the data was obtained when these three bond lengths were assigned separate fitting parameters (α_{fit} and σ^2). Beyond the first shell, there exists no discrete coordination shell as all higher order V-O, V-P and V-V bonds are intertwined. This is the reason why EXAFS data of ε-$LiVOPO_4$ are characterized by the first prominent peak only. Due to the finite data range and therefore, limited number of parameters, all higher order bonds were grouped based on the type of backscattering atoms and constrained under the same fitting parameters. A similar

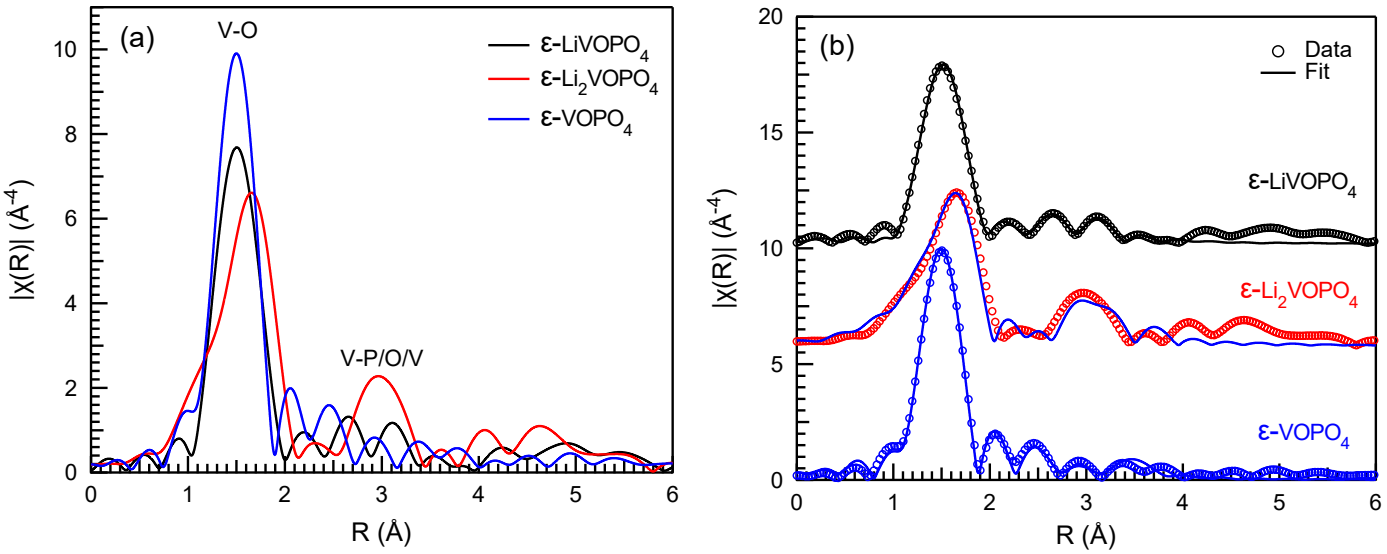

Fig. S3 (a) Fourier-transformed EXAFS signals of chemically prepared, phase pure reference compounds ε-$LiVOPO_4$, ε-Li_4VOPO_4 and ε-$VOPO_4$ along with EXAFS fits in (b).

strategy was adapted to fit EXAFS data of triclinic ε-Li_2VOPO_4 (space group: $P\bar{1}$)[6], where V atoms are distributed over two different octahedral sites. The absence of short vanadyl bond in ε-Li_2VOPO_4 shifts the first peak representing the V-O coordination to higher R-values. Moreover, the evolution of peak at $\sim$3 Å is the characteristic EXAFS feature of ε-Li_2VOPO_4 phase. The reappearance of the short vanadyl bond in ε-$VOPO_4$ shifts back the first peak toward lower R-values. However, a relatively higher crystal symmetry of monoclinic ε-$VOPO_4$ (space group: C1c1)[7] with only one octahedral V site (Table S5) gives rise to a local environment with much less intertwining of coordination shells and consequently, more intense EXAFS features. A good agreement between the data and theory for all vanadyl phosphate reference compounds can be seen in Figure S3b.

Table S1 Local structure around V1 atoms of ε-$LiVOPO_4$.

$S_0^2 = 0.9(2)$ ΔE_0 = -10.9(3.6)						
Central absorber	Coordinat. atoms	Degen.	R_{theory} (Å)	α_{fit}	R_{fit} (Å)	σ^2_{fit} (Å^2)
V1	O	1	1.626	-0.003(9)	1.621(13)	0.004(2)
		1	1.968	-0.010(6)	1.948(12)	0.004(2)
		1	1.973		1.953(12)	
		1	1.991		1.971(12)	
		1	2.029		2.008(12)	
		1	2.240	0.036(23)	2.321(52)	0.011(6)
	P	1	3.156	-0.009(7)	3.128 (22)	0.005(3)
		1	3.200		3.171(22)	
		1	3.273		3.244(23)	
	O	1	3.297	-0.005(17)	3.281(56)	0.009(10)
	P	1	3.382	-0.009(7)	3.352(24)	0.005(3)
	V	1	3.599	0.004(9)	3.613(32)	0.009(3)
	O	1	3.606	-0.005(17)	3.588(61)	0.009(10)
	V	1	3.629	0.004(9)	3.644(33)	0.009(3)
	O	1	3.682	-0.005(17)	3.664(63)	0.009(10)
		1	3.691		3.673(63)	
		1	3.700		3.682(63)	
		1	3.797		3.778(65)	
		1	3.837		3.818(65)	
		1	3.897		3.878(66)	
		1	3.907		3.887(66)	
		1	4.050		4.030(69)	
		1	4.148		4.127(71)	
		1	4.198		4.177(71)	

Table S2 Local structure around V2 atoms of ε-$LiVOPO_4$.

$S_0^2 = 0.9(2)$ ΔE_0 = -10.9(3.6)						
Central absorber	Coordinat. atoms	Degen.	R_{theory} (Å)	α_{fit}	R_{fit} (Å)	σ^2_{fit} (Å^2)
V2	O	1	1.627	-0.003(9)	1.622(13)	0.004(2)
		1	1.944	-0.010(6)	1.925(12)	0.004(2)
		1	1.983		1.963(12)	
		1	1.984		1.964(12)	
		1	2.016		1.996(12)	
		1	2.240	0.036(23)	2.320(51)	0.011(6)
	P	1	3.226	-0.009(7)	3.197(23)	0.005(3)
		1	3.250		3.221(23)	
		1	3.298		3.268(23)	
		1	3.303		3.273(23)	
	O	1	3.342	-0.005(17)	3.325(57)	0.009(10)
		1	3.498		3.481(59)	
	V	1	3.599	0.004(9)	3.613(32)	0.009(3)
		1	3.629		3.644(33)	
	O	1	3.631	-0.005(17)	3.613(62)	0.009(10)
		1	3.670		3.652(62)	
		1	3.719		3.700(63)	
		1	3.812		3.793(65)	
		1	3.977		3.957(68)	
		1	4.005		3.985(68)	
		1	4.109		4.088(70)	
		1	4.168		4.147(71)	
		1	4.178		4.157(71)	
		1	4.206		4.185(72)	

Table S3 Local structure around V1 atoms of ε-Li_2VOPO_4.

$S_0^2 = 0.8(2)$ ΔE_0 = -8.5(4.4)						
Central absorber	Coordinat. atoms	Degen.	R_{theory} (Å)	α_{fit}	R_{fit} (Å)	σ^2_{fit} (Å^2)
V1	O	1	1.921	0.003(22)	1.927(42)	0.004(7)
		1	1.954		1.960(43)	
		1	2.033	0.002(12)	2.036(24)	0.001(4)
		1	2.058		2.062(25)	
		1	2.097		2.101(25)	
		1	2.099		2.103(25)	
	P	1	3.323	0.000(29)	3.323(96)	0.004(37)
		1	3.335		3.335(97)	
		1	3.450		3.45(10)	
	V	1	3.514	-0.003(12)	3.503(42)	0.003(8)
	P	1	3.523	0.000(29)	3.52(10)	0.004(37)
	O	1	3.577	0.027(23)	3.674(82)	0.004(8)
	V	1	3.589	-0.003(12)	3.578(43)	0.003(8)
	O	1	3.612	0.027(23)	3.710(83)	0.004(8)
		1	3.846		3.950(88)	
		1	3.848		3.952(89)	
		1	3.888		3.993(89)	
		1	3.949		4.056(91)	
		1	3.991		4.099(92)	

Table S4 Local structure around V2 atoms of ε-Li_2VOPO_4.

$S_0^2 = 0.8(2)$ ΔE_0 = -8.5(4.4)						
Central absorber	Coordinat. atoms	Degen.	R_{theory} (Å)	α_{fit}	R_{fit} (Å)	σ^2_{fit} (Å^2)
V2	O	1	1.935	0.003(22)	1.941(43)	0.004(7)
		1	1.940		1.945(43)	
		1	1.964		1.970(43)	
		1	2.045	0.002(12)	2.049(25)	0.001(4)
		1	2.070		2.074(25)	
		1	2.168		2.172(26)	
	P	1	3.172	0.000(29)	3.172(92)	0.004(37)
		1	3.310		3.310(96)	
		1	3.394		3.394(98)	
		1	3.461		3.46(10)	
	O	1	3.496	0.027(23)	3.590(80)	0.004(8)
	V	1	3.514	-0.003(12)	3.503(42)	0.003(8)
	O	1	3.520	0.027(23)	3.615(81)	0.004(8)
	V	1	3.589	-0.003(12)	3.578(43)	0.003(8)
	O	1	3.656	0.027(23)	3.755(84)	0.004(8)
		1	3.696		3.796(85)	
		1	3.767		3.869(87)	
		1	3.885		3.990(89)	

Table S5 Local structure around V atoms of ε-$VOPO_4$.

$S_0^2 = 0.8(2)$ ΔE_0 = -4.1(3.4)						
Central absorber	Coordinat. atoms	Degen.	R_{theory} (Å)	α_{fit}	R_{fit} (Å)	σ^2_{fit} (Å^2)
V	O	1	1.572	0.004(6)	1.578(9)	0.002(1)
		1	1.838	0.009(6)	1.855(11)	0.003(1)
		1	1.861		1.878(11)	
		1	1.882		1.899(11)	
		1	1.920		1.937(12)	
		1	2.556	-0.074(37)	2.367(95)	0.013(14)
	P	1	3.184	0.001(7)	3.187(22)	0.008(4)
		1	3.201		3.204(22)	
		1	3.215		3.218(23)	
		1	3.308		3.311(23)	
	O	1	3.473	0.029(8)	3.574(28)	0.000(3)
		1	3.650		3.756(29)	
		1	3.677		3.784(29)	
		1	3.784		3.894(30)	
		1	3.794		3.904(30)	

Table S6 Statistical EXAFS fitting parameters for ε-$LiVOPO_4$ samples discharged/charged using different rates.

Conditions	State of Cathode	Δk (Å^{-1})	ΔR (Å)	N_{idp}	N_{vary}	ν	χ^2	χ^2_ν	R
C/10	Pristine	3.3 - 11.0	1.0 - 4.2	15	14	1	7	5	0.00004
	Dis.1.6 V	3.1 - 12.3	1.0 - 4.3	19	12	7	12988	1779	0.002
	Chg.3.5 V	3.3 - 11.0	1.0 - 4.3	16	13	3	318	118	0.00002
	Chg.4.5 V	3.3 - 12.2	1.1 - 4.0	16	13	3	267	88	0.0001
C/20 + 10h CV	Dis.1.6 V	3.1 - 12.2	1.0 - 4.4	19	12	7	5763	793	0.002
	Chg.3.5 V	3.3 - 11.0	1.0 - 4.2	16	13	3	225	75	0.00004
	Chg.4.5 V	3.3 - 12.0	1.0 - 4.0	16	13	3	5	2	0.00007
C/50	Dis.1.6 V	3.1 - 10.9	1.0 - 4.4	16	12	4	12247	2640	0.002
	Chg.3.5 V	3.3 - 11.0	1.0 - 4.1	15	13	2	17	8	0.00001
	Chg.4.5 V	3.6 - 12.2	1.0 - 4.0	16	13	3	292	92	0.0007
C/100	Dis.1.6 V	3.1 - 10.9	1.0 - 4.4	16	12	4	2632	566	0.002
	Chg.3.5 V	3.3 - 11.2	1.0 - 4.0	15	13	2	226	110	0.0001
	Chg.4.5 V	3.5 - 12.2	1.0 - 4.0	16	13	3	6481	1822	0.0008
Ref.	$LiVOPO_4$	3.3 - 12.2	1.01 - 4.0	17	14	3	420	152	0.00005
	Li_2VOPO_4	3.1 - 12.2	1.0 - 4.3	19	12	7	17641	2551	0.002
	$VOPO_4$	3.6 - 12.3	1.0 - 4.0	16	12	4	3414	778	0.00009

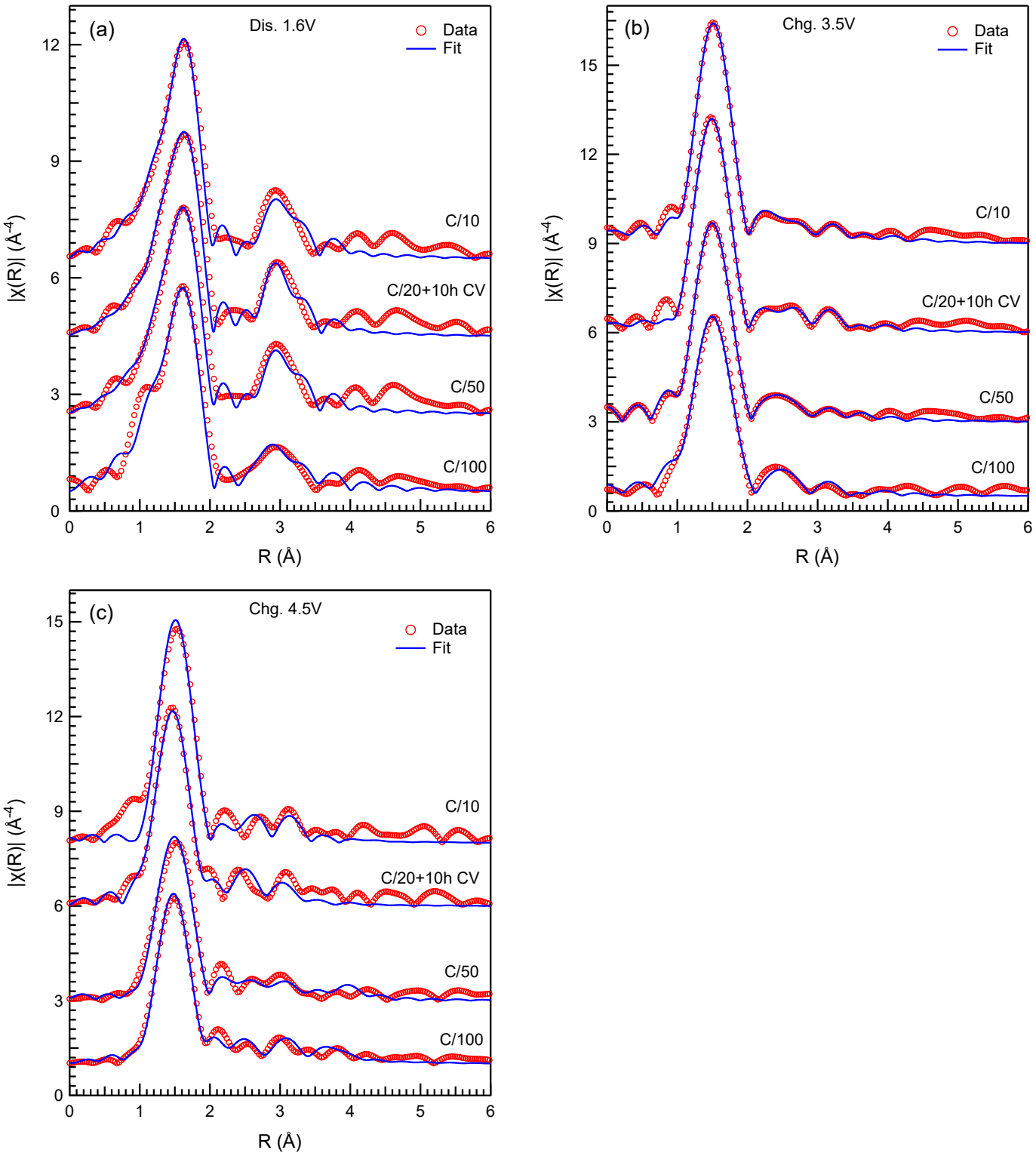

Fig. S4 EXAFS fits to the data of ε-$LiVOPO_4$ samples (a) discharged to 1.6 V (b) recharged to 3.5 V and (c) recharged to 4.5 V using different rates.

Linear-combination fitting (LCF)

LCF was carried out using the software ATHENA. For samples charged to 4.5 V, LCF was performed between 5460 - 5475 eV using the pristine material and ε-$VOPO_4$ as endmember references. For discharged samples, LCF was carried out between 5464 - 5471 eV using the pristine material and ε-Li_2VOPO_4 as endmember references. The sum of the refined fractions of endmember references was constrained to 1 and threshold energy (i.e.) was allowed to vary in LCF. A good agreement between the data and fit for all discharged/charged samples can be seen in Figure S5

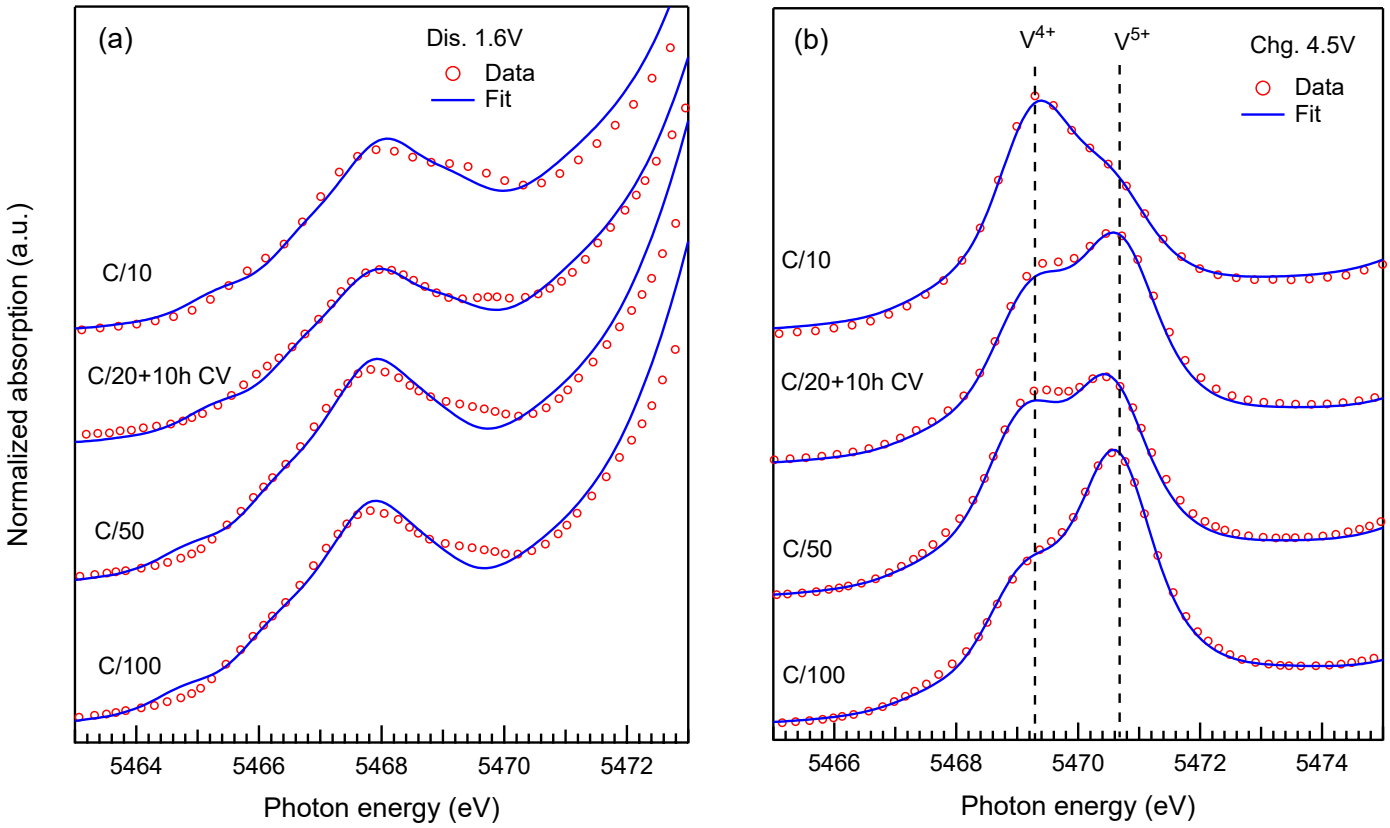

Fig. S5 Linear-combination fits to the pre-edge region of ε-$LiVOPO_4$ samples (a) discharged to 1.6 V and (b) charged to 4.5 V using different rates.

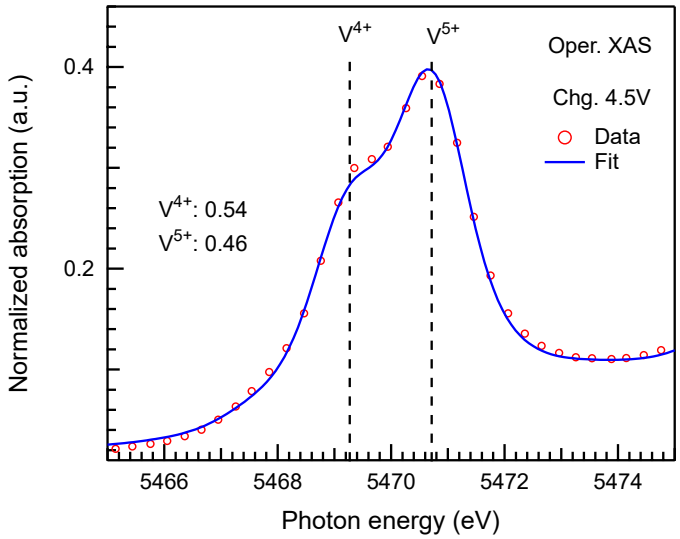

Fig. S6 Linear-combination fit to the pre-edge region of ε-$LiVOPO_4$ charged to 4.5 V at C/4 during operando XAS measurements.

Notes and references

1 A. Lavrov, V. Nikolaev, G. Sadikov and M. Porai Koshits, *Dokl. Akad. Nauk SSSR*, 1982, **266**, 343–346.

2 J. Rehr, E. Stern, R. Martin and E. Davidson, *Phys. Rev. B*, 1978, **17**, 560–565.

3 E. Stern, B. Bunker and S. Heald, *Phys. Rev. B*, 1980, **21**, 5521–5539.

4 B. Teo, *EXAFS: Basic principles and data analysis*, Springer-Verlag Berlin, 1986, vol. 10.

5 S. Calvin, *PhD thesis*, The City University of New York, 2001.

6 M. Bianchini, J. Ateba-Mba, P. Dagault, E. Bogdan, D. Carlier, E. Suard, C. Masquelier and L. Croguennec, *J. Mater. Chem. A*, 2014, **2**, 10182.

7 F. Girgsdies, W. Dong, J. Bartley, G. Hutchings, R. Schlögl and T. Ressler, *Solid State Sci.*, 2006, **8**, 807–812.